

The role of sky view factor and urban street greenery in human thermal comfort and heat stress in a desert climate

Ahmadi Venhari, Armaghan; Tenpierik, Martin; Taleghani, Mohammad

DOI

[10.1016/j.jaridenv.2019.04.009](https://doi.org/10.1016/j.jaridenv.2019.04.009)

Publication date

2019

Document Version

Accepted author manuscript

Published in

Journal of Arid Environments

Citation (APA)

Ahmadi Venhari, A., Tenpierik, M., & Taleghani, M. (2019). The role of sky view factor and urban street greenery in human thermal comfort and heat stress in a desert climate. *Journal of Arid Environments*, 166, 68-76. <https://doi.org/10.1016/j.jaridenv.2019.04.009>

Important note

To cite this publication, please use the final published version (if applicable). Please check the document version above.

Copyright

Other than for strictly personal use, it is not permitted to download, forward or distribute the text or part of it, without the consent of the author(s) and/or copyright holder(s), unless the work is under an open content license such as Creative Commons.

Takedown policy

Please contact us and provide details if you believe this document breaches copyrights. We will remove access to the work immediately and investigate your claim.

The role of sky view factor and urban street greenery in human thermal comfort and heat stress in a desert climate

Abstract

The aim of this study was to understand the effect of urban street greenery type and arrangements on thermal comfort and heat stress in summer. Field measurements and computer simulations were carried out on East-West (E-W) and North-South (N-S) oriented streets in Isfahan, Iran. Through the field measurements in July 2014, 17 different streets were studied, followed by 15 perturbation scenarios (urban design alternatives) simulated by ENVI-met. The study showed that there is a significant and positive relationship between the Sky View Factor (SVF) and the Physiological Equivalent Temperature (PET) values. Comparison of the meteorological parameters within different street orientations showed that the effect of the SVF on the E-W streets was more significant than in N-S streets. Furthermore, greenery arrangement and building heights showed different impacts on the outdoor thermal comfort streets with different orientations.

Keywords:

Thermal comfort, heat stress, urban greenery, sky view factor, urban streets, desert climate.

1. Introduction

Human thermal comfort represents a state of mind that expresses satisfaction with the thermal environment (ISO-7730, 2005). Traditional thermal comfort theory was based on the balance between heat production and heat loss to keep the core body temperature at around 37 °C (Nikolopoulou and Lykoudis, 2006, Van Hoof, 2008). As thermal comfort is affected by different environmental factors like air temperature, wind speed, humidity and mean radiant temperature, it requires an overall view of human-biometeorological conditions. Thermal comfort consists of six factors; two personal (metabolic rate (Met) and thermo-physical properties of clothing (Clo)); and four environmental factors (air temperature (T_a), mean radiant temperature (T_{mrt}), air velocity (V_a) and relative humidity (RH)) (Mayer, 1993).

There are different human-biometeorological indexes. Physiological Equivalent Temperature (PET) has been used in several studies to evaluate the human thermal comfort in outdoor environments (Höppe, 1999, Mayer and Höppe, 1987). Several advantages are associated with the popularity of PET, like involving clothing and metabolic rate in the calculations, and using °C as a tangible unit of measurement (Deb and Alur, 2010). In a desert climate with high air temperature and low humidity in summertime, the human-biometeorological conditions not only cause discomfort, but also severe heat stress could happen for pedestrians. It means that the body cannot maintain its core temperature at around 37 °C, which is harmful for elderly and people with cardiovascular problems (Sampson et al., 2013, Robine et al., 2008, Kabisch et al., 2017).

Several heat mitigation strategies are used to decrease thermal stress and improve thermal comfort in urban areas. Adding urban greenery is one of the well-known strategies (Vanos et al., 2019, Saaroni et al., 2018, Lee et al., 2016, Lee and Mayer, 2018). As mentioned in many studies, shading (Shashua-Bar and Hoffman, 2000, Kotzen, 2003, Saaroni et al., 2018, Mayer et al., 2008, Holst and Mayer, 2011, Lee et al., 2013, Lee et al., 2014), evaporation (Montazeri et al., 2015), and transpiration (Fryd et al., 2011, Oliveira et al., 2011, Taleghani, 2018) cause the cooling effect of urban greenery. In contrast to the urban heat island effect, the term “Urban Cool Island” (UCI) is used when an area in a city is cooled down by a heat mitigation strategy like urban greenery (Hamada and Ohta, 2010). When the cooling effect is due to urban greenery, the term Green Cooling Island (GCI) is used (Taha et al., 2016). Yang et al. (2011) studied the effect of urban design strategies on thermal comfort. They observed PET reduction up to 20 °C under the shadow of casting trees above pavements. In Sao Paulo, a reduction in PET of up to 12 °C was found due to street greenery (Spangenberg et al., 2008). Toudert and Mayer (2007) reported a reduction in PET of more than 20 °C. Furthermore, climate is an important factor that determines GCI. The effectiveness of urban greenery is more appreciable in hot climates (Shashua-Bar and Hoffman, 2002, Bowler et al., 2010). In a recent study in Iraq, the results showed that shading by trees increased the outdoor thermal comfort dramatically (Ridha et al., 2018). Two studies in 2017 presented that the GCIs in arid and semi-arid climates are more effective than other climates. Furthermore, the number of studies in these climates are limited (Ahmadi Venhari et al., 2017, Kleerekoper et al., 2017).

69 Iran has diverse climates. There are limited days in a year which meet thermal comfort
70 conditions (Daneshvar et al., 2013). Roshan et al. (2017) determined new threshold
71 temperatures for cooling and heating degree days index for different parts of Iran. The results
72 showed that southern coasts and central plateau of Iran have more Cooling Degree Days (CDD)
73 and need maximum cooling energy. One of the passive design strategies recommended in such
74 climates is human-biometeorological oriented design (Snir et al., 2016, Middel et al., 2019,
75 Taleghani et al., 2019, Zamani et al., 2012). Solar radiation, wind speed and evaporation are
76 three important factors of climate design in such desert climates. Greenery is one of the most
77 effective elements of a human-biometeorological oriented design which plays an important role
78 in improving thermal comfort (Middel et al., 2015, Taleghani and Berardi, 2018, Lee et al.,
79 2016, Lee and Mayer, 2018). There are many studies that showed the heat mitigation impacts
80 of vegetation in traditional courtyards (Foruzanmehr and Vellinga, 2011, Nasrollahi et al.,
81 2017, Taleghani et al., 2012), and in urban scale (Akbari and Kolokotsa, 2016, Yan et al., 2018)
82 in arid climates. Due to the water shortage in such climates, urban greenery needs to be
83 designed in the most efficient way.

84

85 Urban streets occupy the largest areas among urban spaces in cities (Jacobs, 1961). This is
86 more common in compact cities like Iranian cities. Greening such large areas could
87 significantly alter the urban climate. The main objective of this study is to understand how to
88 design urban greenery for N-S and E-W streets. A previous study in Cuba illustrated that the
89 heat stress is not the same in streets with different directions. In E-W streets, the heat stress
90 was more than other directions (Rodríguez-Algeciras et al., 2018). There are several methods
91 to find the most effective amount of shading trees. One of the most popular ones is based on
92 the calculation of the sky view factor (SVF). SVF is defined as the percentage of free sky at a
93 specific location (Oke, 2002), which ranges from 0 (completely obstructed) to 1 (completely
94 open to the sky). By adding buildings and vegetation, the view to the sky could be blocked. As
95 many studies illustrated, decreasing the SVF can reduce air temperature during the day
96 (Svensson, 2006, Unger, 2004, Lee et al., 2014). Similar results show a direct relationship
97 between SVF and PET in winter and summer (Lin et al., 2010, Charalampopoulos et al., 2013).
98 This study will answer the following questions:

99

- 100 - What is the effect of green SVF and built SVF on pedestrian thermal comfort (based
101 on the direction of streets)?
- 102 - What is the effect of SVF on streets in Isfahan?
- 103 - What greenery arrangement is more effective for E-W streets and N-S streets?
- 104 - How is the importance of the shading greenery in comparison with non-shading
105 greenery on thermal comfort?

106

107 **2. Methodology**

108 This paper studies the effect of urban street greenery on pedestrians' thermal comfort. As
109 mentioned in the introduction, different micrometeorological parameters influence thermal
110 comfort like air temperature (T_a), mean radiant temperature (T_{mrt}), relative humidity (RH) and
111 wind speed as well as personal factors. This study used PET as the thermal comfort index. The

112 effect of the built environment (height to width ratio in street canyons; H/W), urban greenery
113 and SVF on thermal comfort were studied. The amount of green coverage was calculated from
114 satellite images. For the ENVI-met simulations, building SVF and tree SVF were reported,
115 separately. SVF was calculated with the RayMan software package (Matzarakis et al., 2010,
116 Lee and Mayer, 2016). Lee and Mayer (2016) discussed that several studies have validated T_{mrt}
117 with RayMan; however, these studies are mainly based on simulations. In their study, they
118 validated RayMan results for T_{mrt} and PET with measured data for the first time (Lee and
119 Mayer, 2016). They could show that RayMan “satisfactorily” simulates T_{mrt} under
120 homogeneous conditions; however, the accuracy decreases with lower solar elevation.
121

122 **2.1.The study area**

123 The historical city of Isfahan is one of the largest cities in Iran with a population of 1.9
124 million in 493.8 km². Local latitude is 32°65'N, longitude 51°66'E and the elevation is
125 approximately 1590 m above sea level. Isfahan has a desert climate (Köppen-Geiger BWk)
126 with high air temperature and low humidity during the summer, and cold desert climate in
127 winter (Kottek et al., 2006). This climate is also known as an arid climate, as the precipitation
128 is between 25 to 200mm per year. Desert climates divide to hot desert climate (BWh- like
129 Tucson (Arizona) and Cairo (Egypt)), and cold desert climate (BWk like central Iranian cities
130 like Isfahan, and Santiago (Chile)). Yaghmaei et al. (2009) studied the human-
131 biometeorological conditions of Isfahan province based on Köppen (2006) climate
132 classification. These methods have been compared and a multivariate statistical method has
133 been suggested. They showed that the city of Isfahan has a windy, arid and warm climate.
134 Based on global warming and some wrong decisions in water management in Iran, Isfahan has
135 been confronted with drought and the main river of the city, Zayandehrood, has dried up. By
136 comparing the mean monthly temperature of July 2000 till 2015, the increase in air temperature
137 over the last decade is more than 3°C (geographic.org, 2017).
138

139 **2.2. Field study**

140 To select the streets for this study, a surface temperature map was prepared by Envi 4.7 based
 141 on the Landsat 7 data (Figure 1). As a result, 4 districts were chosen. The hottest district in the

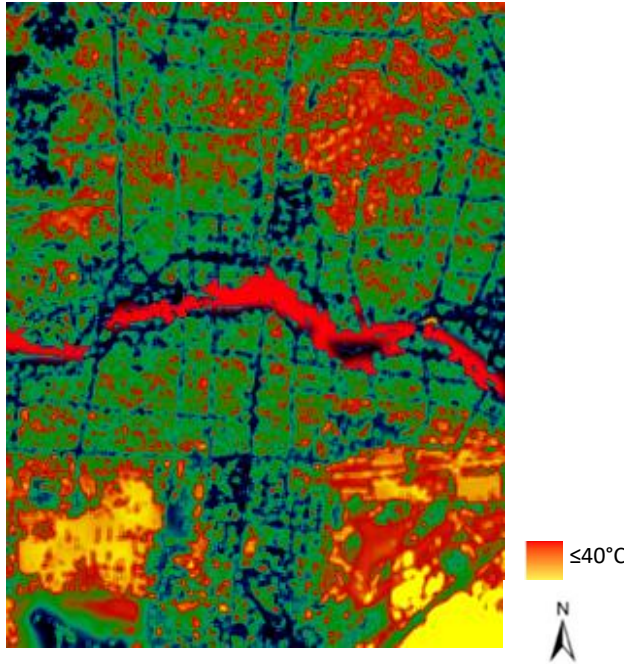


Figure 1: Thermal surface simulation of Isfahan,

20 July 2013



Figure 2: The location of selected districts for field study in the city of Isfahan

142 historical fabric (Dis 1); the coolest district (Dis 2); and two other districts, one in a new fabric
 143 and another located between the old and the new fabric in Isfahan. Figure 2 shows the selected
 144 districts. In each district, 3 to 8 streets were chosen with either N-S or E-W streets. The streets
 145 have different amounts of urban greenery, H/W and greenery arrangements (Table 2). In
 146 District 2, the number of selected streets is more than the other districts due to the existing
 147 different greenery arrangements. Based on the method which has been applied by Shashua-
 148 Bar and Hoffman (2002), in each street several points with a distance of about 20 m were
 149 studied. To make the data comparable, a reference point was selected in each district. This
 150 reference point did not have any vegetation or shading during the day. Data were not collected
 151 during the windy days. The wind velocity was less than 0.5 m/s in all days during which data
 152 was gathered. Measurements were performed from 20th to 25th July 2014 at 8:00, 13:00, 17:00
 153 and 22:00 at the height of 1.4 m above the ground. Table 1 presents the specification of the
 154 measurement devices. A black globe with diameter equal to 15 cm was used to measure T_g .
 155 T_{mrt} was then calculated by Equation 1 (ISO7726, 1998):

156

$$157 \quad T_{mrt} = \left[(T_g + 273.15)^4 + 2.5 \cdot 10^8 \cdot V_a^{0.6} (T_g - T_a) \right]^{1/4} - 273.15 \quad (1)$$

158

159 where;

160 T_{mrt} is mean radiant temperature,

161 T_g is globe temperature,

162 V_a is wind speed, and

163 T_a is air temperature.

164

165

Table 1: Devices used in the field studies.

Variable	Unit	Devices	Accuracy	Method of storage	Calibrated company	Applied points
Air Temperature (T_a)	°C	Kestrel 4500	0.1°C±	Automatic	Kestrel Meters	Reference points
		Kimo-VT100-1	0.3°C±	Manual	KIMO instrument	Site measurements
		Heat index WBGT meter 8758	0.6°C±	Manual	UMTC	Site measurements
Humidity	%	EasyLog. EL-USC-2-LCD	±3%	Automatic	Lascar Electronics	Reference point and Site measurements
Wind Velocity	m/s	Kimo-VT100-1	0.05±	Manual	KIMO instrument	Site measurements
		Kestrel 4500	0.1±	Manual	Kestrel Meters	Site measurements
Globe Temperature (T_g)	°C	Heat index WBGT meter 8758	1.5°C±	Manual	UMTC	Site measurements
Surface Temperature (T_s)	°C	Infrared FLIR E4 Camera	-	Automatic	FLIR instrument	Site measurements

167

168 In each point of the streets, a fish eye photo was taken. A Sony Cyber Shot DSC-H7 with

169 42xHD lens and 800dpi resolution was employed to take the fish eye photos. By inputting these

170 fish eye photos and other meteorological data in RayMan 1.2, the SVF and PET were

171 calculated. For each street, the differences between the observation points and the reference

172 points are represented by ΔT_a , ΔT_s , ΔT_{mrt} , and ΔPET .

173



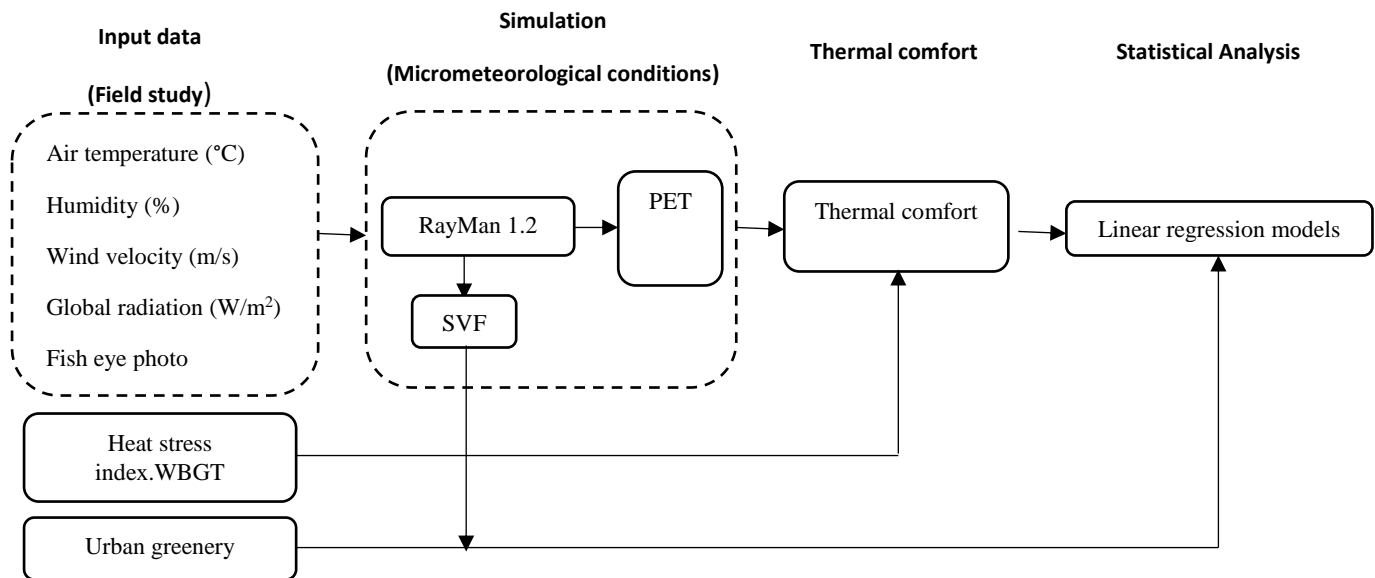
174

175

Figure 3: Devices used in the field study.

176

177 Figure 4 illustrates the research method used for the field studies.



179

180

181

182

Figure 4: Research method in field study

Table 2: Site data and measurement plan.

District	Street	Number of observation points	Street direction	Green coverage (%)	Average SVF	Width of streets(m)	
1	Abdorazzagh	30	N-S	19	0.67	35	
	Hatef	21	N-S	27	0.56	25	
	Moshirodole	16	E-W	0	0.62	15	
2	Cheharbagh. A	30	N-S	67	0.41	43	
	Shaykh Bahai	21	E-W	38.5	0.59	20	
	Shams Abadi	21	N-S	34	0.61	25	
	Alam Ala	15	E-W	91	0.33	12	
	Amadegah	18	E-W	37	0.46	20	
	Bagh Goldaste	21	N-S	1	0.82	35	
	Niasarm	21	E-W	94	0.22	20	
	Abas Abad	18	E-W	82	0.28	15	
	3	Shaykh sadugh	24	N-S	58	0.58	35
		Azadi	42	E-W	42	0.6	30
Freiburg		28	N-S	11	0.76	35	
4	Daghighi	18	E-W	9	0.73	35	
	Nayej	18	N-S	85	0.54	20	
	Khaghani	18	E-W	25	0.41	15	

183

2.2.Simulation

In stage 2 of the research, ENVI-met 3.1 was employed (Bruse, 2004, Bruse and Fler, 1998). This software is used for three dimensional micrometeorological simulations. Its typical spatial resolution is between 0.5 to 10m. ENVI-met simulates air and surface temperatures ($^{\circ}\text{C}$), relative humidity (%), wind velocity (m/s) and mean radiant temperature ($^{\circ}\text{C}$) (Bruse, 2019). Fluid dynamics and thermodynamics are the bases to simulate heat, vapour and air flows at different levels. The grid size used for the simulations were $2 * 2 * 2 \text{ m}^3$ (x * y * z). ENVI-met has been previously used in different studies that focused on urban greenery (Wong et al., 2007, Fabbri et al., 2017, Lee and Mayer, 2016, Lee and Mayer, 2018).

In this stage of the study, five different alternatives were simulated (Alt1 to Alt5 shown in Figure 5). These alternatives had different amounts and arrangements of greenery in a 25 m wide street in Isfahan. Meteorological data of the 4th district was used as the input because of the common form of its streets in Isfahan. In addition, these five alternatives were studied for three different heights of the adjacent buildings: H/W equal to 1/1, 1/2, 1/4.

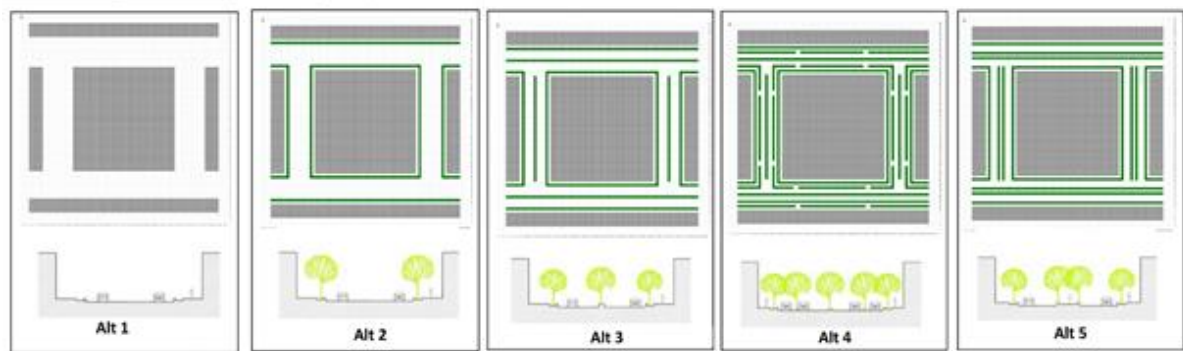


Figure 5: Five alternatives with different amount and arrangements of greenery which have been simulated in ENVI-met.

For each simulation, four receptors in the E-W and four receptors in the N-S streets recorded the simulated meteorological data. Fifteen simulation scenarios with 16 receptors (in each model) were run for a 24-hour period during the 20th of July 2014. Meteorological data at the height of 1.4 m from receptors were extracted (like the measurement campaign). This height was chosen as it is closest to the human body core (Ali-Toudert and Mayer, 2006). In addition, the first alternative scenario without greenery was considered as the reference model. PET reduction for each alternative is calculated from the average PET differences of the receptor

209 points in the simulation models. Figure 6 illustrates a summary of the research method for the
 210 simulations.

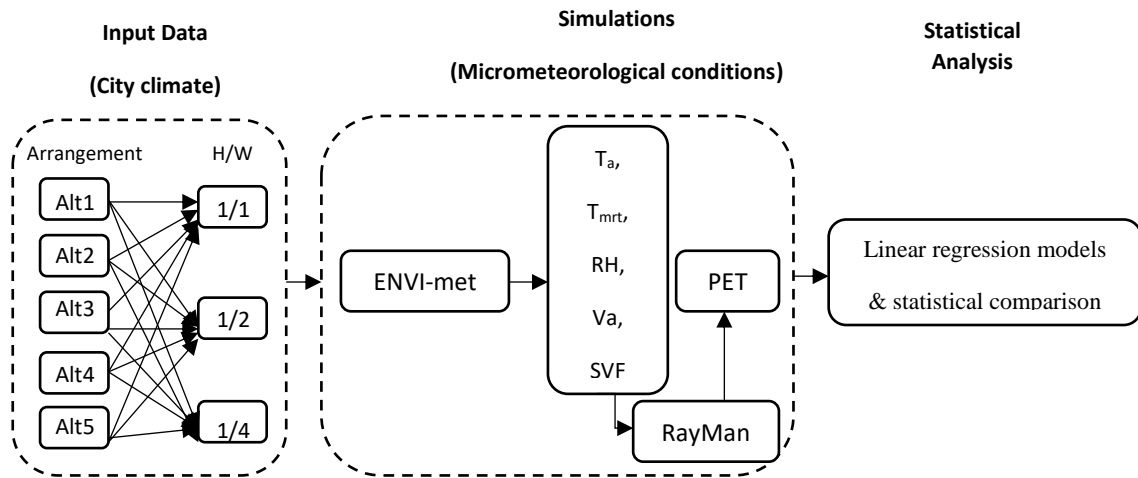


Figure 6: Research method in simulations.

211

212

213 3. Results and discussion:

214 3.1. The effect of sky view factor (SVF) on thermal comfort

215 To find out the amount of solar radiation within urban spaces, linear regression analyses were
 216 done between the different GCI parameters and SVF. Table 5 presents the average differences
 217 of T_a , T_s , T_{mrt} and PET between the measurement points and the reference points that have been
 218 used in the regression analyses.

219

220

Table 3: The average difference of thermal indexes between measurement points and the reference point

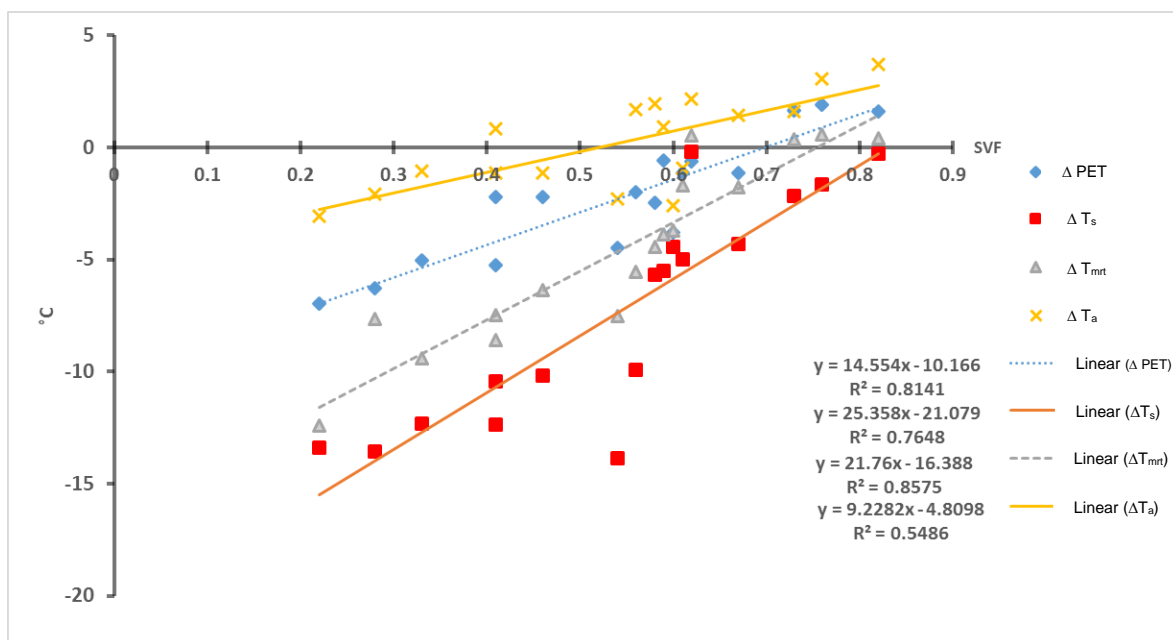
221

ΔPET (°C)	ΔT_{mrt} (°C)	ΔT_s (°C)	ΔT_a (°C)	Street	District
1.4	-4.3	-1.8	1.1	Abdorazzagh	1
1.7	-9.9	-5.6	2.0	Hatef	
2.2	-0.2	0.5	0.6	Moshirodole	
-1.1	-10.4	-7.5	-2.2	Cheharbagh. A	2
0.9	-5.5	-3.9	-0.6	Shaykh Bahai	
-0.9	-5	-1.7	1.1	Shams Abadi	
-1.1	-12.3	-9.4	-5.0	Alam Ala	
-1.1	-10.2	-6.4	-2.2	Amadegah	
3.7	-0.3	0.4	1.6	Bagh Goldaste	
-3.1	-13.4	12.4	-7.0	Niasarm	3
-2.1	-13.6	-7.6	-6.3	Abas Abad	
2.0	-5.7	-4.5	-1.4	Shaykh sadugh	
-2.6	-4.4	-3.7	3.8	Azadi	
3.1	-1.7	0.6	1.9	Fribourg	4
1.6	-2.2	0.4	1.6	Daghighi	
-2.3	-13.9	-7.5	-4.5	Nayej	
0.8	-12.4	-8.6	6.3	Khaghani	

231 First, all streets regardless of their direction were included in the analysis to see the effect of
 232 SVF on ΔT_a , ΔT_s , ΔT_{mrt} and ΔPET . As can be seen in Figure 6, the effect of SVF on air
 233 temperature is not appreciable, however, its effect on thermal comfort (PET), T_s and T_{mrt} is
 234 notable. Because of other factors like land use, the limited effect of SVF on T_a is explainable.

235 For example, in Azadi street, a park is near the street which affects the ambient air temperature.
 236 Because of these factors, the coefficient of determination (R^2) for this relationship is also
 237 smallest (54%). This means that 54% of the variations in ΔT_a is explained by the corresponding
 238 variations in SVF. The largest effect of SVF was found on ΔT_s , with a slope of the regression
 239 line of 23.6 °C per unit change in SVF ($R^2=0.71$), which means that the direct effect of SVF on
 240 surface temperatures. The largest coefficient of determination was found between ΔT_{mrt} and
 241 SVF ($R^2=0.84$). This indicates that 84% of the variations in ΔT_{mrt} is explained by changes in
 242 the SVF. Due to the intense solar radiation in desert climates, the necessity of controlling solar
 243 radiation availability can be clearly seen. Furthermore, it was observed that minimum (0.22)
 244 and maximum (0.82) SVF led to 10.2°C difference in PET. In addition, the results of the
 245 regression analyses show a significant positive relationship between SVF and PET.

246



247 Figure 7: The linear regression model for the relation between SVF and thermal indexes without street direction.

248

249 The next part of the comparison is focused on the street directions. As Table 6 presents, based
 250 on the slope of the regression lines (b), the SVF affects the air temperature in N-S streets more
 251 than in E-W ones. In addition, PET is more affected by SVF in E-W streets than in N-S ones.
 252 In general, PET was higher in E-W streets compared to the N-S streets. Decreasing SVF has a
 253 stronger cooling effect (on PET) in E-W streets. This is in accordance with the previous studies
 254 that showed the effectiveness of shading from urban greenery (Shashua-Bar and Hoffman,
 255 2000, Holst and Mayer, 2011, Lee et al., 2016, Lee and Mayer, 2018).

256

257

258

259

260 Table 4: Results of regression analysis between thermal indexes and SVF based on direction (a is intercept; b is slope; r is
 261 correlation coefficient).

Direction	N-S			E-W		
	a	b	r	a	b	R

262
263
264
265

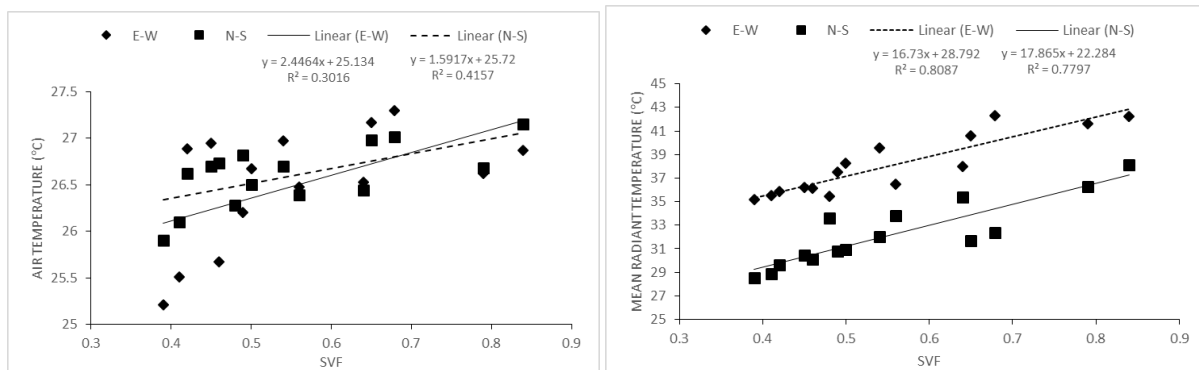
ΔT_a (°C)	-6.948	12.805	0.76	-4.08	7.7725	0.64
ΔT_s (°C)	-19.809	26.266	0.93	-23.554	28.509	0.83
ΔT_{mrt} (°C)	-15.978	22.918	0.93	-16.938	22.15	0.91
ΔPET (°C)	-9.2476	13.31	0.82	-10.12	14.947	0.92

266

267 The ENVI-met results showed that the effect of the SVF on air temperature was smaller than
 268 its effect on other micrometeorological factors. A 0.1 unit increase in SVF led to an increase
 269 of 1.6 °C and 2.4 °C air temperature in N-S and E-W streets, respectively. The effect of the
 270 SVF on T_{mrt} was found to be stronger (Figure 7). A 0.1 unit increase in SVF led to 17.9 °C and
 271 16.7 °C increase of mean radiant temperature within N-S and E-W streets, respectively. Among
 272 different micrometeorological parameters, mean radiant temperature was more affected by
 273 changing the amount of greenery. The effect of the SVF on T_{mrt} in E-W streets seems to be
 274 quite similar to N-S streets. In general, T_{mrt} is about 6.0 °C higher in streets with E-W
 275 orientation than in streets with N-S orientation (with equal SVF). The reason can be that E-W
 276 streets are insolated from early morning, and they warm up sooner than N-S streets.

277 As the regression model illustrates (Figure 8), the effect of SVF on thermal comfort can
 278 emphasise the importance of shading. Shading trees and the shadow of buildings are very
 279 effective in this climate.

280



281
282

283 Figure 8: The regression model of the cooling effect of SVF with street direction based on simulations.

284

285

286

287 3.2 The cooling effect of street greenery arrangement, H/W ratio, and Greenery 288 arrangement

289

290 To explore the cooling effect of different street greenery arrangements, RayMan was used
 291 to calculate the PET after the ENVI-met simulations. Comparing the different greenery
 292 arrangements, the maximum GCI (in PET) was 13.6 °C. This shows the important role of
 293 greenery arrangements in providing outdoor thermal comfort. To understand the cooling effect

294 of different alternatives, average PET was compared. Alt 1 (with no greenery) was used as the
 295 reference model. By adding shading trees (Figure 9), 4 °C reduction in the average PET was
 296 observed. In N-S streets, the difference between Alt-2 with two lines of greenery, and Alt 3
 297 with three lines of greenery was about 0.6 °C. This PET reduction in E-W streets is 1.5 °C. It
 298 can be concluded that adding shading trees at the middle of the E-W streets is an effective
 299 arrangement to improve the pedestrians' thermal comfort. The most effective alternative for
 300 both directions is Alt 4 which is dividing the streets into different lines for pedestrians,
 301 transition and traffic with in-between shading trees. As a result, in desert climates a lower SVF
 302 with streets divided by shading trees is an effective method to improve outdoor thermal
 303 comfort.

304

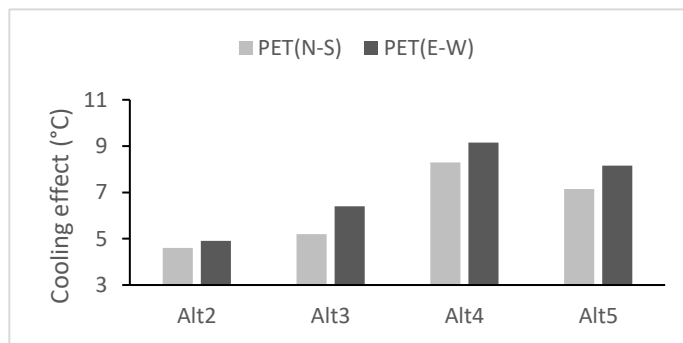


Figure 9: The cooling effect of studied alternatives in simulations, based on the average of PET.

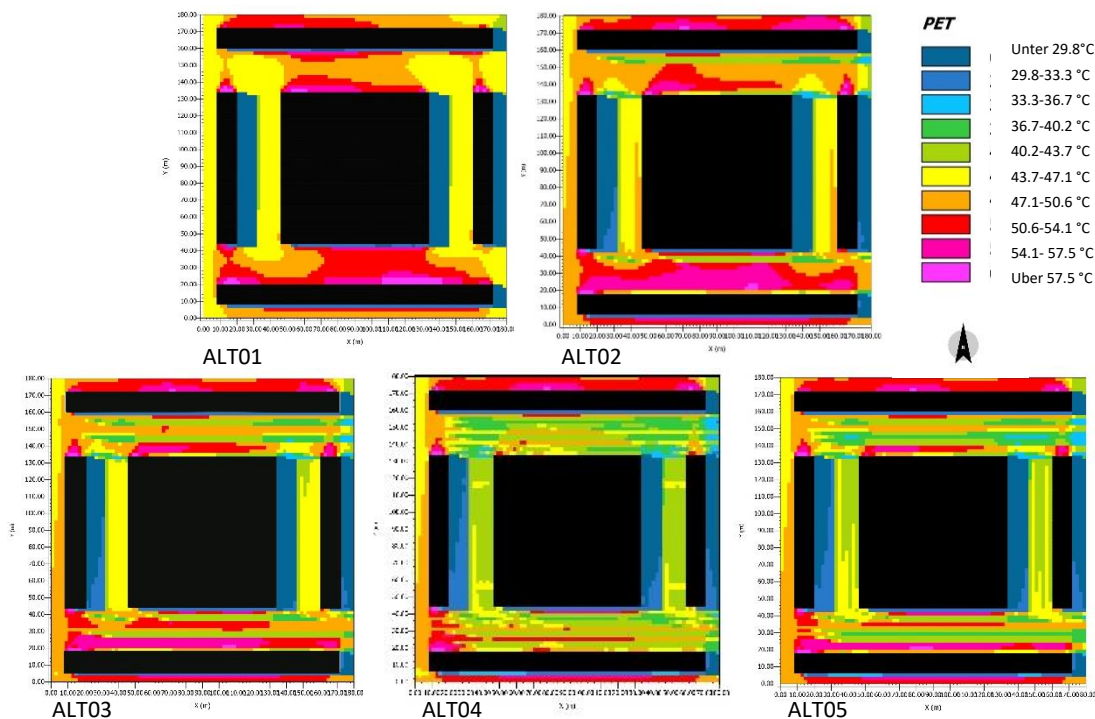


Figure 10: An example of PET simulations by ENVI-met in 13:00 (figures are generated by Leonardo, a component of ENVI-met).

305

306 **Type of greenery:** Trees have a stronger impact on PET reduction than grass. For example,
 307 Freiburg street can be divided into two parts. Both parts have three lines of greenery, but the

308 first part is with shading trees; and the second part is with grass on two sides, and grass and
 309 bushes in the middle. Figure 11 shows the change in air temperature as compared to the bare
 310 reference for 28 measurement points along the street. As the figure shows, the cooling effect
 311 of the first part (lower receptor numbers), especially at around noon, is more than of the second
 312 part (higher receptor numbers). E, W and C represent the east, west and centre of the street.
 313 The results show the importance of shadow in this desert climate. Considering the water
 314 shortage, shading trees play more important role in improving the thermal comfort than non-
 315 shading vegetation.

316

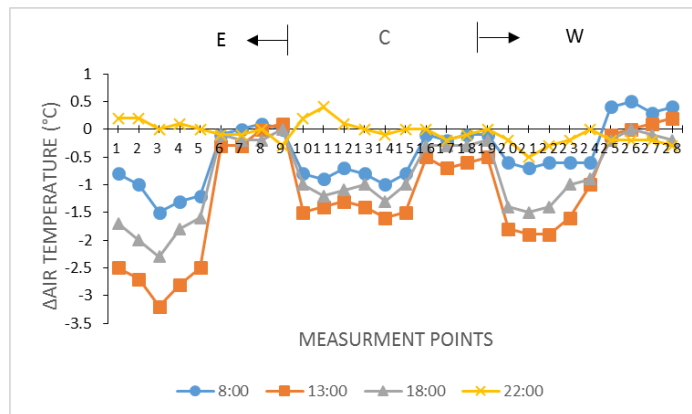


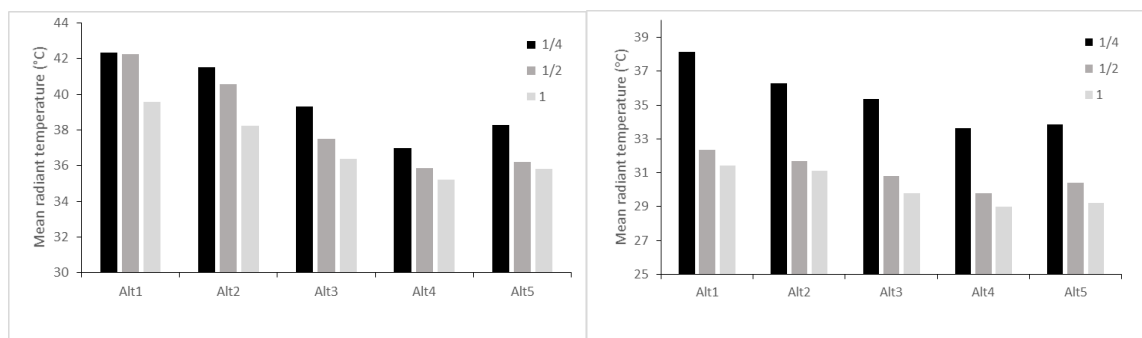
Figure 11: The cooling effect of urban greenery in the middle and two sides of the street.

317

318

319 **H/W ratio:** Simulating different alternatives for three different building heights was the
 320 last part of this study. Figure 12 shows the results of mean radiant temperature in 15
 321 simulations. As the figure shows, increasing the H/W ratio in N-S streets is more effective than
 322 in E-W streets. In N-S streets, by increasing the H/W ratio from 1/4 to 1/2, a maximum
 323 reduction in T_{mrt} of about 14.4 °C was achieved, while the maximum effect in E-W streets was
 324 4.3 °C. The effect of increasing the H/W ratio from 1/4 to 1/2 was more significant than
 325 changing it from 1/2 to 1. Therefore, the recommended H/W ratio for the N-S streets is around
 326 1/2. This result showed that blocking about half of the sky is very effective for heat mitigation.
 327 It should be noted that in N-S streets, blocking more than 1/2 of the sky not only has a small
 328 cooling effect but also may decrease natural ventilation in the streets.

329



330

Figure 12: T_{mrt} in five different H/W scenarios in N-S (left) and E-W streets (right).

331

332 4. Conclusions

333 This study investigated urban street greenery as a strategy to reduce heat stress and to improve
334 thermal comfort in outdoor environments. Field studies and computer simulations were carried
335 out. The analyses were based on the local meteorological conditions of Isfahan in July 2014.
336 In this climate, water shortage is a problem. Finding strategies which help landscape and urban
337 designers take the most efficient decisions was the aim of this research. The effect of SVF,
338 street greenery arrangement and H/W ratio of streets on heat mitigation were studied with
339 different scenarios. The orientations of the investigated streets were North-South and East-
340 West. The main findings of the paper are presented as follow:

- 341 • In the first phase of this study, the relation between the SVF and different
342 micrometeorological factors were studied through field measurements. A regression
343 analysis showed that the effect of SVF on air temperature was smallest, while its effect
344 on mean radiant temperature and surface temperature were the largest. In addition, a
345 positive and significant relationship was obtained between SVF and PET.
- 346 • A comparison of the effect of the greenery types illustrated that not all greenery lead to
347 the same cooling effect. The maximum cooling effect is caused by the shadow of trees.
348 Long lines of grass and bushes are not recommended for the arid climate of Isfahan.
349 Shading trees which their crown cover each other are the most effective forms of
350 greenery to reduce SVF, and consequently PET.
- 351 • Comparing the minimum (0.22) and maximum (0.82) SVFs, led to 10.2 °C difference
352 in PET. In addition, sky obstruction in E-W streets reduced PET more than in N-S
353 streets. This means that not every street needs the same amount of greenery. In E-W
354 streets, controlling the incoming solar radiation is very important.
- 355 • Different alternatives of greenery arrangement led to maximum 13.7 °C reduction in
356 PET. This showed the effect of greenery arrangement on outdoor thermal comfort. In
357 addition, dividing streets into different lines with shading trees has the highest effect
358 for heat stress mitigation. In E-W streets, a row of trees in the centre of the street is very
359 effective to improve the pedestrian's thermal comfort. In addition, increasing the height
360 of the buildings in the N-S streets plays an important role in heat stress mitigation. This
361 effect was not notable in the E-W streets. As a result, increasing greenery in the E-W
362 streets, and increasing the H/W ratio in the N-S streets are the two main recommended
363 strategies for desert climates.

364

365

366 References

- 367 AHMADI VENHARI, A., TENPIERIK, M. & MAHDIZADEH HAKAK, A. 2017. Heat mitigation by greening
368 the cities, a review study. *Environment, Earth and Ecology*, 1, 5-32.
- 369 AKBARI, H. & KOLOKOTSA, D. 2016. Three decades of urban heat islands and mitigation technologies
370 research. *Energy and Buildings*, 133, 834-842.
- 371 ALI-TOUDERT, F. & MAYER, H. 2006. Numerical study on the effects of aspect ratio and orientation of
372 an urban street canyon on outdoor thermal comfort in hot and dry climate. *Building and
373 Environment*, 41, 94-108.

374 ALI-TOUDERT, F. & MAYER, H. 2007. Effects of asymmetry, galleries, overhanging façades and
375 vegetation on thermal comfort in urban street canyons. *Solar Energy*, 81, 742-754.

376 BOWLER, D. E., BUYUNG-ALI, L., KNIGHT, T. M. & PULLIN, A. S. 2010. Urban greening to cool towns
377 and cities: A systematic review of the empirical evidence. *Landscape and Urban Planning*, 97,
378 147-155.

379 BRUSE, M. 2004. ENVI-met 3.0: Updated Model Overview. [http://www.envi-
380 met.net/documents/papers/overview30.pdf](http://www.envi-

380 met.net/documents/papers/overview30.pdf).

381 BRUSE, M. 2019. *ENVI-met website* [Online]. Available: <http://www.envimet.com> [Accessed].

382 BRUSE, M. & FLEER, H. 1998. Simulating surface–plant–air interactions inside urban environments
383 with a three dimensional numerical model. *Environmental Modelling & Software*, 13, 373-
384 384.

385 CHARALAMPOPOULOS, I., TSIROS, I., CHRONOPOULOU-SERELI, A. & MATZARAKIS, A. 2013. Analysis
386 of thermal bioclimate in various urban configurations in Athens, Greece. *Urban Ecosystems*,
387 16, 217-233.

388 DANESHVAR, M. R. M., BAGHERZADEH, A. & TAVOUSHI, T. 2013. Assessment of bioclimatic comfort
389 conditions based on Physiologically Equivalent Temperature (PET) using the RayMan Model
390 in Iran. *Central European Journal of Geosciences*, 5, 53-60.

391 DEB, C. & ALUR, R. 2010. *The significance of Physiological Equivalent Temperature (PET) in outdoor
392 thermal comfort studies*.

393 FABBRI, K., CANUTI, G. & UGOLINI, A. 2017. A methodology to evaluate outdoor microclimate of the
394 archaeological site and vegetation role: A case study of the Roman Villa in Russi (Italy).
395 *Sustainable Cities and Society*, 35, 107-133.

396 FORUZANMEHR, A. & VELLINGA, M. 2011. Vernacular architecture: questions of comfort and
397 practicability. *Building Research & Information*, 39, 274-285.

398 FRYD, O., PAULEIT, S. & BÜHLER, O. 2011. The role of urban green space and trees in relation to
399 climate change. *CAB Reviews: Perspectives in Agriculture, Veterinary Science, Nutrition and
400 Natural Resources*, 6, 1-18.

401 GEOGRAPHIC.ORG. 2017. Available:
402 [https://geographic.org/global_weather/iran/esfahan_shahid_beheshti_intl_408000_99999.
403 html](https://geographic.org/global_weather/iran/esfahan_shahid_beheshti_intl_408000_99999.html) [Accessed 15.01.2017].

404 HAMADA, S. & OHTA, T. 2010. Seasonal variations in the cooling effect of urban green areas on
405 surrounding urban areas. *Urban Forestry & Urban Greening*, 9, 15-24.

406 HOLST, J. & MAYER, H. 2011. Impacts of street design parameters on human-biometeorological
407 variables. *Meteorologische Zeitschrift*, 20, 541-552.

408 HÖPPE, P. 1999. The physiological equivalent temperature - A universal index for the
409 biometeorological assessment of the thermal environment. *International Journal of
410 Biometeorology*, 43, 71-75.

411 ISO7726 1998. International Standard 7726. *Ergonomics of the thermal environment - Instrument for
412 measuring physical quantities*. Geneva: ISO

413 ISO-7730 2005. ISO 7730 2005-11-15 Ergonomics of the Thermal Environment: Analytical
414 Determination and Interpretation of Thermal Comfort Using Calculation of the PMV and PPD
415 Indices and Local Thermal Comfort Criteria. ISO.

416 JACOBS, J. 1961. *The Death and Life of Great American Cities*, Vintage Books.

417 KABISCH, N., VAN DEN BOSCH, M. & LAFORTEZZA, R. 2017. The health benefits of nature-based
418 solutions to urbanization challenges for children and the elderly – A systematic review.
419 *Environmental Research*, 159, 362-373.

420 KLEEREKOPER, L., TALEGHANI, M., VAN DEN DOBBELSTEEN, A. & HORDIJK, T. 2017. Urban measures
421 for hot weather conditions in a temperate climate condition: A review study. *Renewable and
422 Sustainable Energy Reviews*, 75, 515-533.

423 KOTTEK, M., GRIESER, J., BECK, C., RUDOLF, B. & RUBEL, F. 2006. World Map of the Köppen-Geiger
424 climate classification updated. *Meteorologische Zeitschrift*, 15, 259-263.

425 KOTZEN, B. 2003. An investigation of shade under six different tree species of the Negev desert
426 towards their potential use for enhancing micro-climatic conditions in landscape
427 architectural development. *Journal of Arid Environments*, 55, 231-274.

428 LEE, H., HOLST, J. & MAYER, H. 2013. Modification of Human-Biometeorologically Significant Radiant
429 Flux Densities by Shading as Local Method to Mitigate Heat Stress in Summer within Urban
430 Street Canyons. *Advances in Meteorology*, 2013, 13.

431 LEE, H. & MAYER, H. 2016. Validation of the mean radiant temperature simulated by the RayMan
432 software in urban environments. *International Journal of Biometeorology*, 60, 1775-1785.

433 LEE, H. & MAYER, H. 2018. Maximum extent of human heat stress reduction on building areas due to
434 urban greening. *Urban Forestry & Urban Greening*, 32, 154-167.

435 LEE, H., MAYER, H. & CHEN, L. 2016. Contribution of trees and grasslands to the mitigation of human
436 heat stress in a residential district of Freiburg, Southwest Germany. *Landscape and Urban
437 Planning*, 148, 37-50.

438 LEE, H., MAYER, H. & SCHINDLER, D. 2014. Importance of 3-D radiant flux densities for outdoor
439 human thermal comfort on clear-sky summer days in Freiburg, Southwest Germany.
440 *Meteorologische Zeitschrift*, 23, 315-330.

441 LIN, T.-P., MATZARAKIS, A. & HWANG, R.-L. 2010. Shading effect on long-term outdoor thermal
442 comfort. *Building and Environment*, 45, 213-221.

443 MATZARAKIS, A., RUTZ, F. & MAYER, H. 2010. Modelling radiation fluxes in simple and complex
444 environments: basics of the RayMan model. *Int J Biometeorol*, 54, 131-9.

445 MAYER, H. 1993. Urban bioclimatology. *Experientia*, 49, 957-963.

446 MAYER, H., HOLST, J., DOSTAL, P., FLORIAN, I. & SCHINDLER, D. 2008. Human thermal comfort in
447 summer within an urban street canyon in Central Europe. *Meteorologische Zeitschrift*, 17,
448 241-250.

449 MAYER, H. & HÖPPE, P. 1987. Thermal comfort of man in different urban environments. *Theoretical
450 and Applied Climatology*, 38, 43-49.

451 MIDDEL, A., CHHETRI, N. & QUAY, R. 2015. Urban forestry and cool roofs: Assessment of heat
452 mitigation strategies in Phoenix residential neighborhoods. *Urban Forestry & Urban
453 Greening*, 14, 178-186.

454 MIDDEL, A., LUKASCZYK, J., ZAKRZEWSKI, S., ARNOLD, M. & MACIEJEWSKI, R. 2019. Urban form and
455 composition of street canyons: A human-centric big data and deep learning approach.
456 *Landscape and Urban Planning*, 183, 122-132.

457 MONTAZERI, H., BLOCKEN, B. & HENSEN, J. L. M. 2015. Evaporative cooling by water spray systems:
458 CFD simulation, experimental validation and sensitivity analysis. *Building and Environment*,
459 83, 129-141.

460 NASROLLAHI, N., HATAMI, M., KHASTAR, S. R. & TALEGHANI, M. 2017. Numerical evaluation of
461 thermal comfort in traditional courtyards to develop new microclimate design in a hot and
462 dry climate. *Sustainable Cities and Society*, 35, 449-467.

463 NIKOLOPOULOU, M. & LYKOUDIS, S. 2006. Thermal comfort in outdoor urban spaces: Analysis across
464 different European countries. *Building and Environment*, 41, 1455-1470.

465 OKE, T. R. 2002. *Boundary Layer Climates*, London, Taylor & Francis.

466 OLIVEIRA, S., ANDRADE, H. & VAZ, T. 2011. The cooling effect of green spaces as a contribution to
467 the mitigation of urban heat: A case study in Lisbon. *Building and Environment*, 46, 2186-
468 2194.

469 RIDHA, S., GINESTET, S. & LORENTE, S. 2018. Effect of the Shadings Pattern and Greenery Strategies
470 on the Outdoor Thermal Comfort. *International Journal of Engineering and Technology*, 10,
471 108-114.

472 ROBINE, J.-M., CHEUNG, S. L. K., LE ROY, S., VAN OYEN, H., GRIFFITHS, C., MICHEL, J.-P. &
473 HERRMANN, F. R. 2008. Death toll exceeded 70,000 in Europe during the summer of 2003.
474 *Comptes Rendus Biologies*, 331, 171-178.

- 475 RODRÍGUEZ-ALGECIRAS, J., TABLADA, A. & MATZARAKIS, A. 2018. Effect of asymmetrical street
476 canyons on pedestrian thermal comfort in warm-humid climate of Cuba. *Theoretical and*
477 *Applied Climatology*, 133, 663-679.
- 478 ROSHAN, G. R., FARROKHZAD, M. & ATTIA, S. 2017. Defining thermal comfort boundaries for heating
479 and cooling demand estimation in Iran's urban settlements. *Building and Environment*, 121,
480 168-189.
- 481 SAARONI, H., AMORIM, J. H., HIEMSTRA, J. A. & PEARLMUTTER, D. 2018. Urban Green Infrastructure
482 as a tool for urban heat mitigation: Survey of research methodologies and findings across
483 different climatic regions. *Urban Climate*, 24, 94-110.
- 484 SAMPSON, N. R., GRONLUND, C. J., BUXTON, M. A., CATALANO, L., WHITE-NEWSOME, J. L., CONLON,
485 K. C., O'NEILL, M. S., MCCORMICK, S. & PARKER, E. A. 2013. Staying cool in a changing
486 climate: Reaching vulnerable populations during heat events. *Global Environmental Change*,
487 23, 475-484.
- 488 SHASHUA-BAR, L. & HOFFMAN, M. E. 2000. Vegetation as a climatic component in the design of an
489 urban street: An empirical model for predicting the cooling effect of urban green areas with
490 trees. *Energy and Buildings*, 31, 221-235.
- 491 SHASHUA-BAR, L. & HOFFMAN, M. E. 2002. The Green CTTC model for predicting the air
492 temperature in small urban wooded sites. *Building and Environment*, 37, 1279-1288.
- 493 SNIR, K., PEARLMUTTER, D. & ERELL, E. 2016. The moderating effect of water-efficient ground cover
494 vegetation on pedestrian thermal stress. *Landscape and Urban Planning*, 152, 1-12.
- 495 SPANGENBERG, J., SHINZATO, P., JOHANSSON, E. & DUARTE, D. 2008. Simulation of the influence of
496 vegetation on microclimate and thermal comfort in the city of Sao Paulo. *Revista da*
497 *Sociedade Brasileira de Arborização Urbana (REVSBAU)*, 3, 1-19.
- 498 SVENSSON, M. K. 2006. Sky view factor analysis – implications for urban air temperature differences.
499 *Meteorological Applications*, 11, 201-211.
- 500 TAHA, H., WILKINSON, J., BORNSTEIN, R., XIAO, Q., MCPHERSON, G., SIMPSON, J., ANDERSON, C.,
501 LAU, S., LAM, J. & BLAIN, C. 2016. An urban-forest control measure for ozone in the
502 Sacramento, CA Federal Non-Attainment Area (SFNA). *Sustainable Cities and Society*, 21, 51-
503 65.
- 504 TALEGHANI, M. 2018. Outdoor thermal comfort by different heat mitigation strategies- A review.
505 *Renewable and Sustainable Energy Reviews*, 81, 2011-2018.
- 506 TALEGHANI, M. & BERARDI, U. 2018. The effect of pavement characteristics on pedestrians' thermal
507 comfort in Toronto. *Urban Climate*, 24, 449-459.
- 508 TALEGHANI, M., CRANK, P. J., MOHEGH, A., SAILOR, D. J. & BAN-WEISS, G. A. 2019. The impact of
509 heat mitigation strategies on the energy balance of a neighborhood in Los Angeles. *Solar*
510 *Energy*, 177, 604-611.
- 511 TALEGHANI, M., TENPIERIK, M. & DOBBELSTEEN, A. 2012. The Effect of Different Transitional Spaces
512 on Thermal Comfort and Energy Consumption of Residential Buildings. *7th Windsor*
513 *Conference: The changing context of comfort in an unpredictable world Cumberland Lodge*.
514 Windsor, UK: Network for Comfort and Energy Use in Buildings.
- 515 UNGER, J. 2004. Intra-urban relationship between surface geometry and urban heat island: review
516 and new approach. *Climate Research*, 27, 253-264.
- 517 VAN HOOFF, J. 2008. Forty years of Fanger's model of thermal comfort: comfort for all? *Indoor Air*, 18,
518 182-201.
- 519 VANOS, J. K., KOSAKA, E., IIDA, A., YOKOHARI, M., MIDDEL, A., SCOTT-FLEMING, I. & BROWN, R. D.
520 2019. Planning for spectator thermal comfort and health in the face of extreme heat: The
521 Tokyo 2020 Olympic marathons. *Science of The Total Environment*, 657, 904-917.
- 522 WONG, N. H., KARDINAL JUSUF, S., AUNG LA WIN, A., KYAW THU, H., SYATIA NEGARA, T. & XUCHAO,
523 W. 2007. Environmental study of the impact of greenery in an institutional campus in the
524 tropics. *Building and Environment*, 42, 2949-2970.

- 525 YAGHMAEI, L., SOLTANI, S. & KHODAGHOLI, M. 2009. Bioclimatic classification of Isfahan province
526 using multivariate statistical methods. *International Journal of Climatology*, 29, 1850-1861.
- 527 YAN, H., WU, F. & DONG, L. 2018. Influence of a large urban park on the local urban thermal
528 environment. *Science of The Total Environment*, 622-623, 882-891.
- 529 YANG, F., LAU, S. S. Y. & QIAN, F. 2011. Thermal comfort effects of urban design strategies in high-
530 rise urban environments in a sub-tropical climate. *Architectural Science Review*, 54, 285-304.
- 531 ZAMANI, Z., TALEGHANI, M. & HOSEINI, S. B. 2012. Courtyards as solutions in green architecture to
532 reduce environmental pollution. *Energy Education Science & Technology, Part A: Energy
533 Science and Research*, 30, 358-396.
- 534